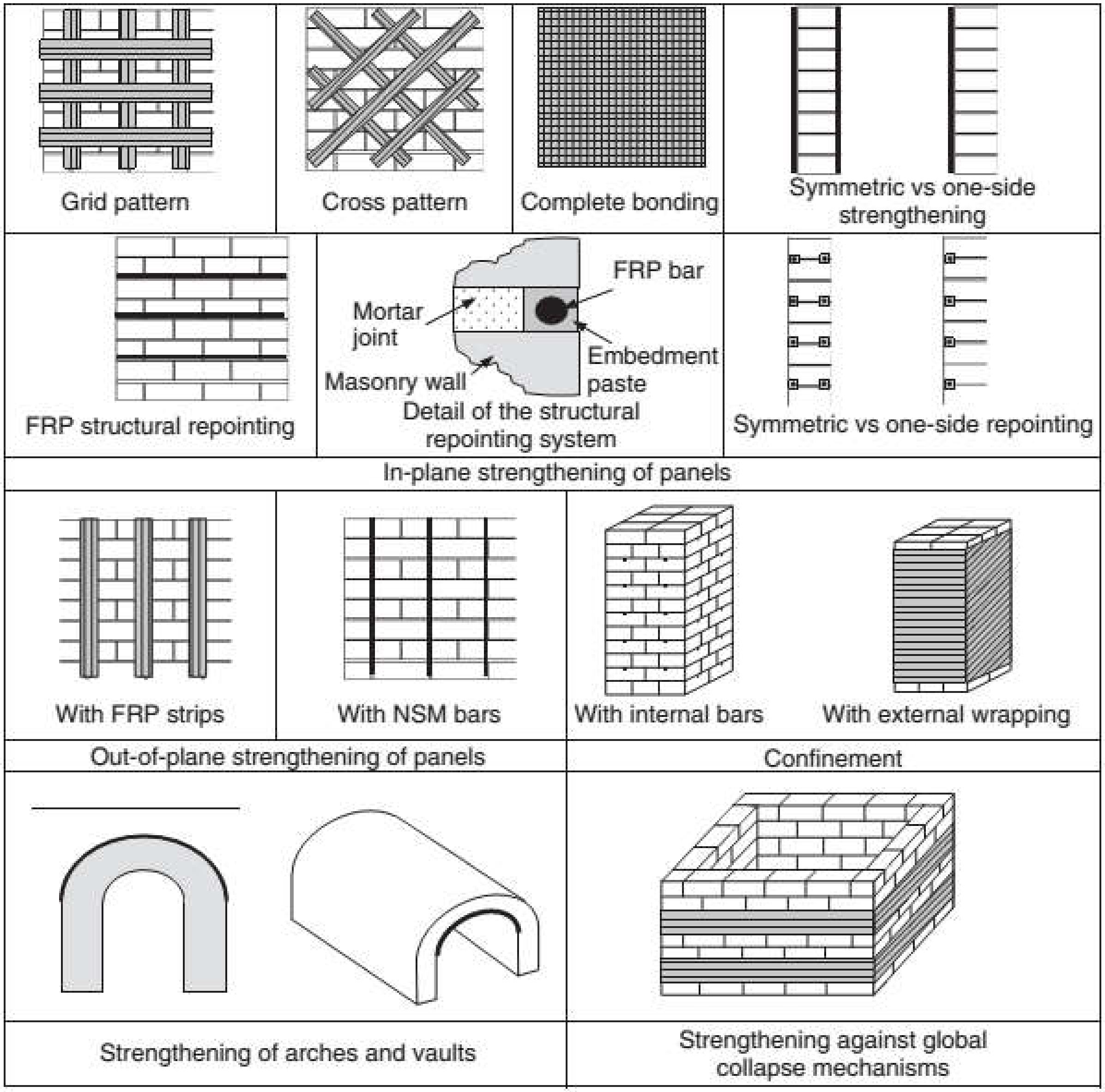

1.3 Example applications of FRP to strengthen masonry members.

Table 2.5 Typical mechanical properties of long directionally aligned fibre–matrix composites (fibre weight fraction 58%) manufactured by the pultrusion technique, (the matrix material is epoxy)

Composite material	Specific weight	Tensile strength (MPa)	Tensile modulus (GPa)	Flexural strength (MPa)	Flexural modulus (Gpa)
E-glass	1.90	750–1050	40.00	1450	40.00
S-2 glass	1.80	1650	55.00	–	–
Aramid 49	1.45	1150–1400	70–110	–	–
Carbon (PAN)	1.60	2670–1950	150–220	1600	–
Carbon (pitch)	1.80	1400–1500	280–350	*Failure strain* $\simeq$ *0.40*	> 330

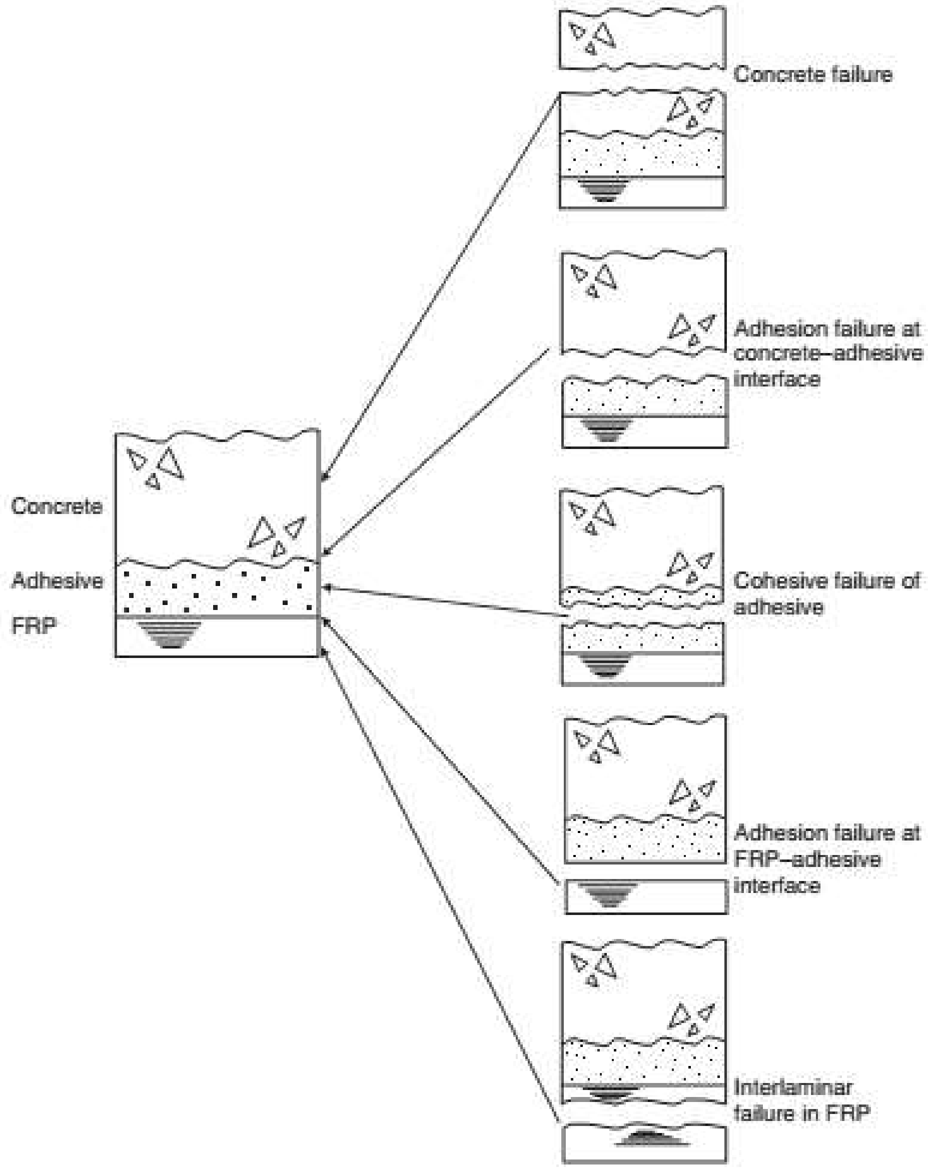

3.5 Possible modes of failure associated with joints comprising FRP adhesively bonded to concrete.

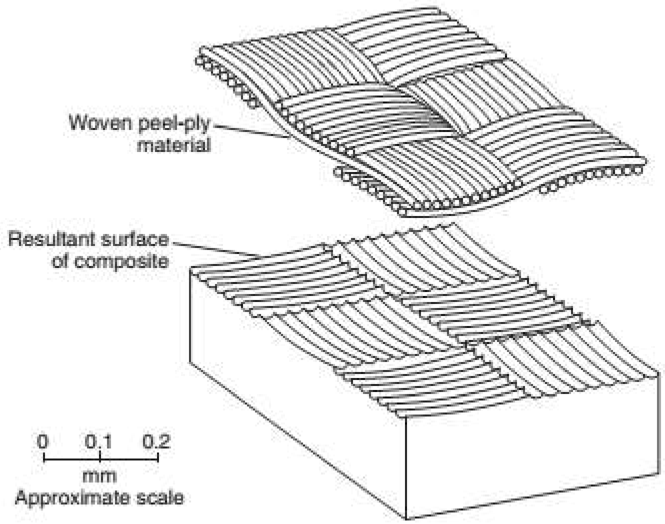

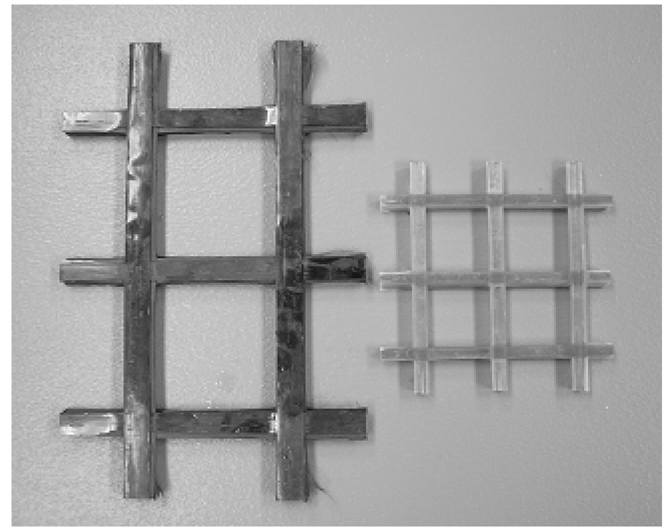

Figure 1.2 NEFMAC FRP grids.

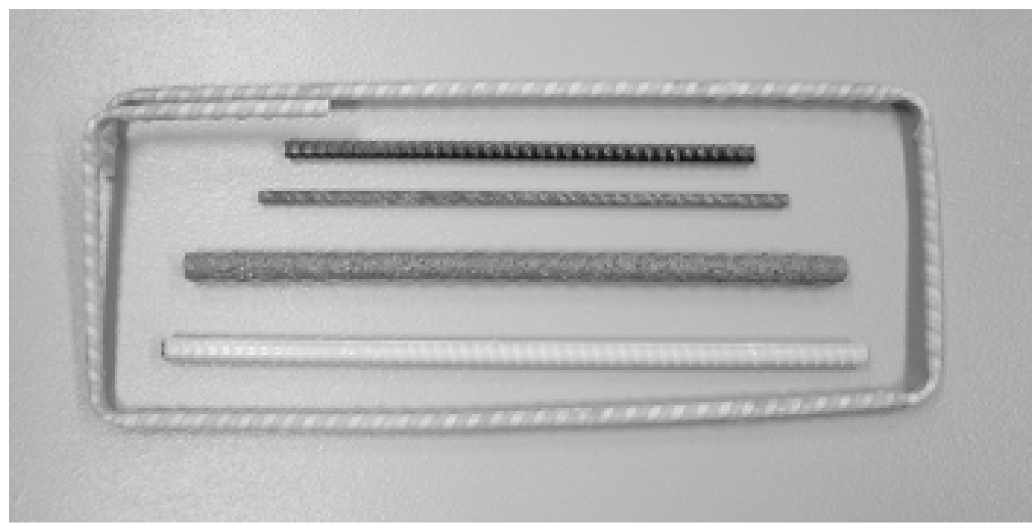

Figure 1.1 Glass- and carbon-reinforced FRP bars.

تقویت تیر

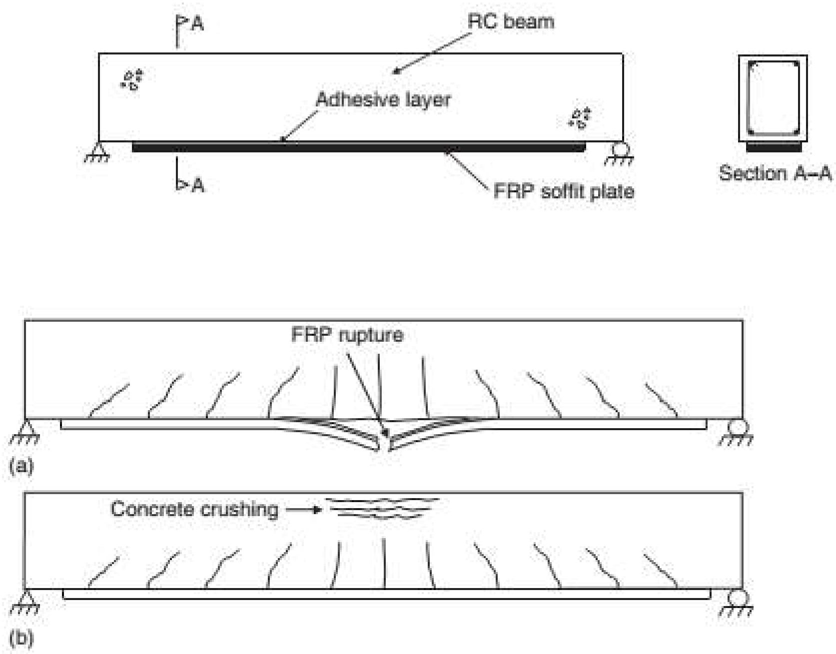

4.2 Conventional flexural failure modes of an FRP-plated RC beam: (a) FRP rupture; (b) crushing of compressive concrete.

type of failure involves a loss of this composite action. Debonding failures generally occur in the concrete, which is also assumed in the design theory presented in this chapter. This is because, with the strong adhesives currently available and with appropriate surface preparation for the concrete substrate, debonding failures along the physical interfaces between the adhesive and the concrete and between the adhesive and the FRP plate are generally not critical.

Debonding may initiate at a flexural or flexural-shear crack in the high moment region and then propagate towards one of the plate ends (Fig. 4.3a). This debonding failure mode is commonly referred to as intermediate crack (IC) induced interfacial debonding (or simply IC debonding) (Teng *et al.*, 2002a, 2003; Lu *et al.*, 2007). Debonding may also occur at or near a plate end (i.e. plate end debonding failures) in four different modes: (i) critical diagonal crack (CDC) debonding (Fig. 4.3b) (Oehlers and Seracino, 2004); (ii) CDC debonding with concrete cover separation (Fig. 4.3c) (Yao and Teng, 2007); (iii) concrete cover separation (Figs 4.3d and 4.3e) (Teng *et al.*, 2002a); and (iv) plate end interfacial debonding (Fig. 4.3f) (Teng *et al.*, 2002a).

مودهای شکست
(Failure Modes)

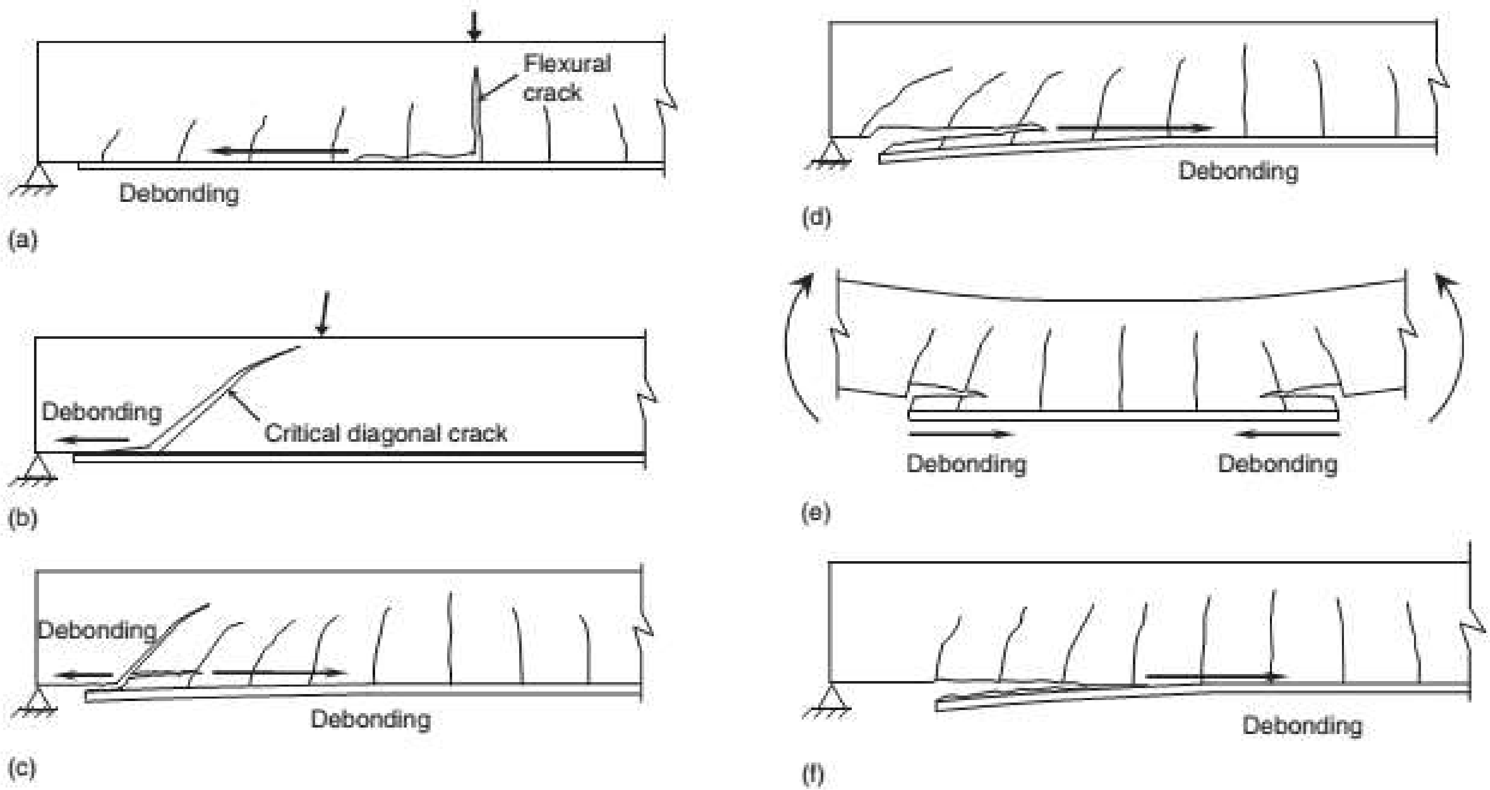

4.3 Debonding failure modes of an FRP-plated RC beam: (a) IC debonding; (b) CDC debonding; (c) CDC debonding with concrete cover separation; (d) concrete cover separation; (e) concrete cover separation under pure bending; (f) plate end interfacial debonding.

مودهای شکست خمشی

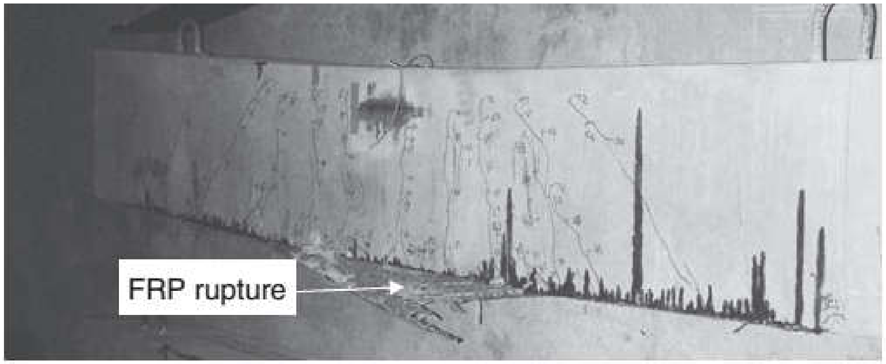

4.4 FRP-plated RC beam: FRP rupture.

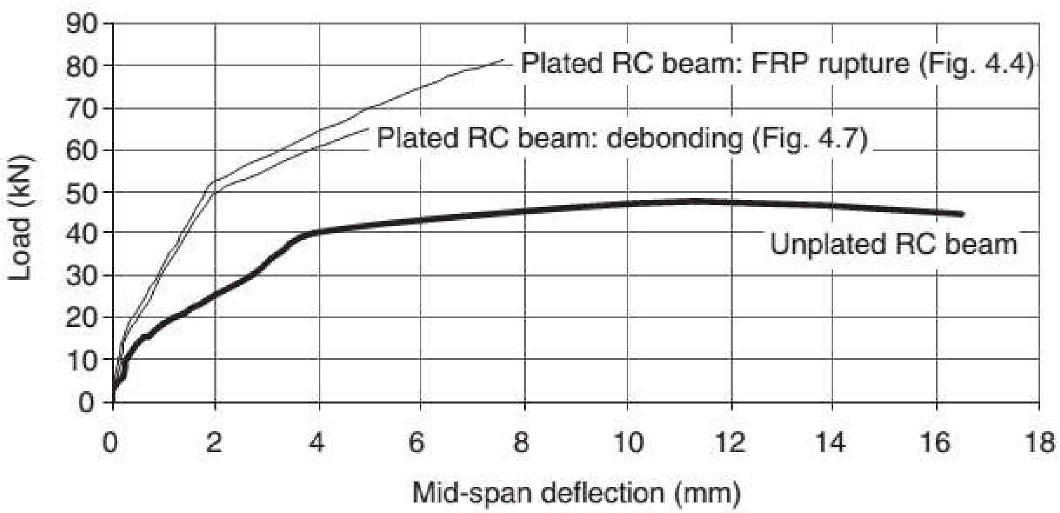

4.5 Typical load–deflection curves of plated and unplated RC beams.

Intermediate crack-induced interfacial debonding

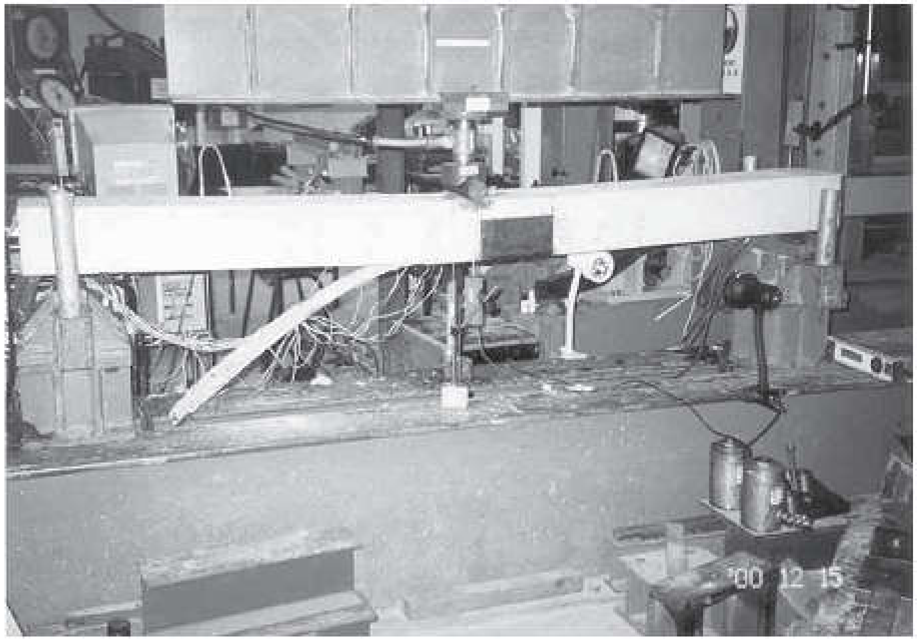

4.6 FRP-plated RC beam: intermediate flexural crack-induced interfacial debonding.

Critical diagonal crack-induced interfacial debonding (CDC debonding)

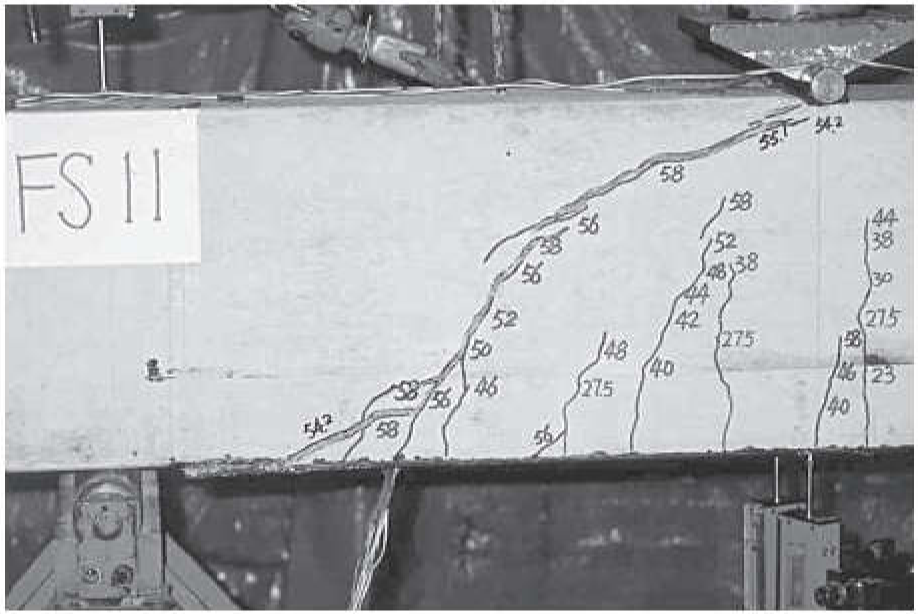

4.9 FRP-plated RC beam: CDC debonding.

Concrete cover separation

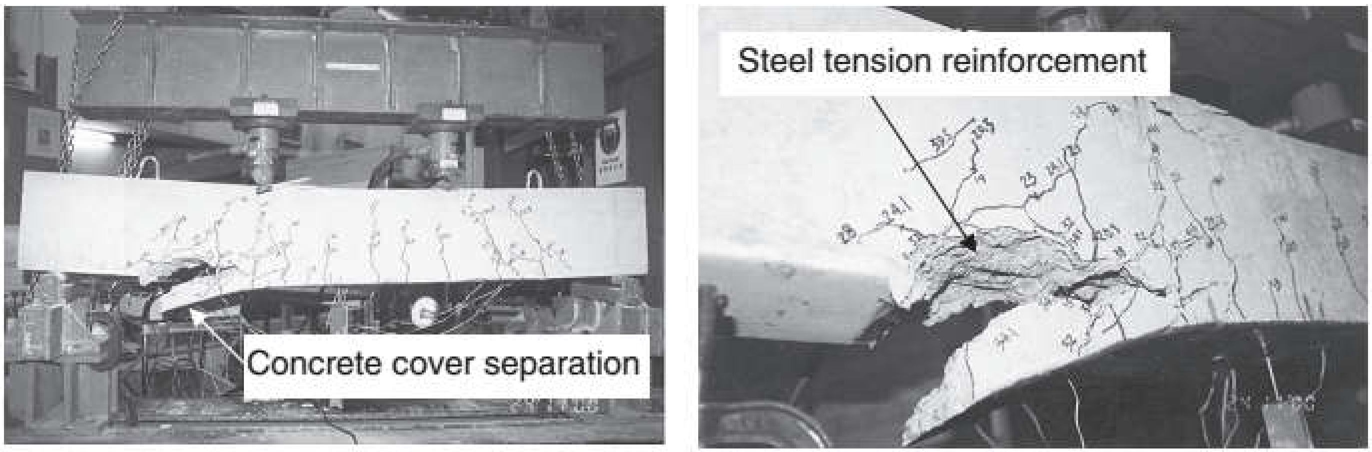

(a) (b)

4.7 FRP-plated RC beam: concrete cover separation: (a) overall view; (b) close-up view.

Plate-end interfacial debonding

4.8 FRP-plated RC beam: plate-end interfacial debonding.

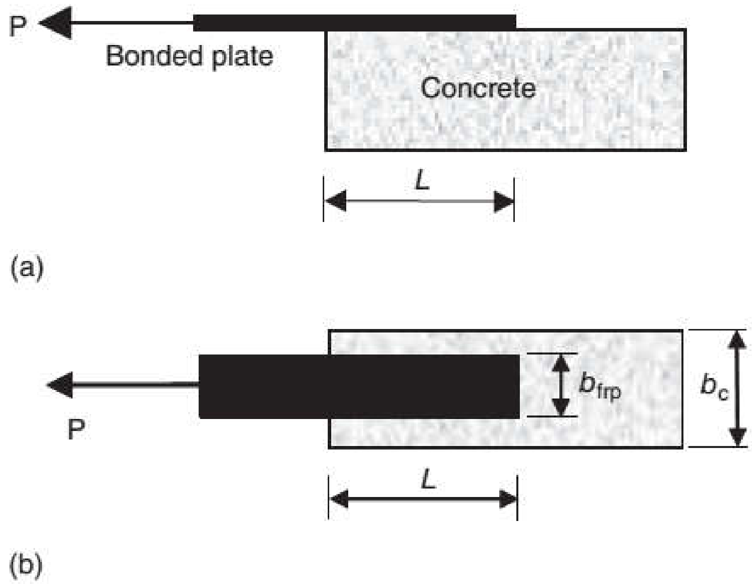

4.15 Schematic of a simple pull-off test: (a) elevation; (b) plan.

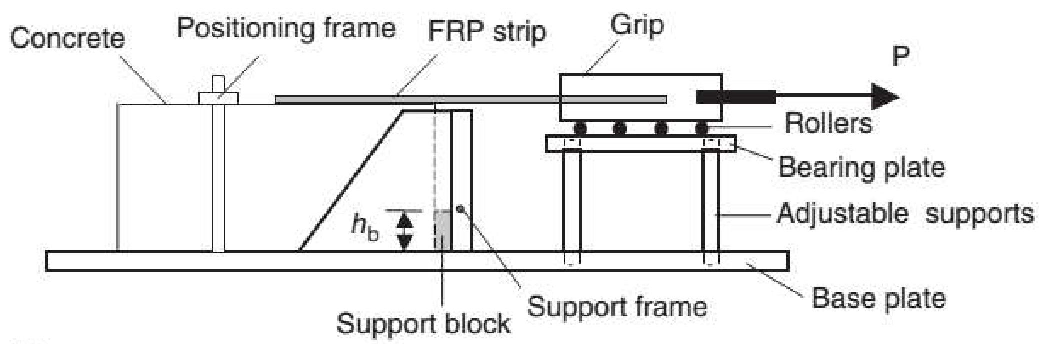

(a)

4.16 Set-up for pull-off tests

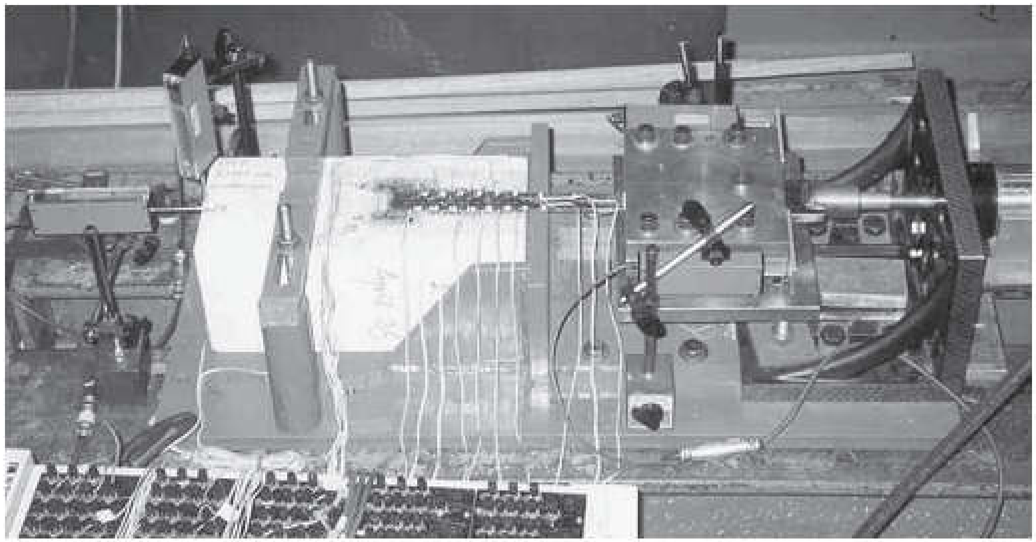

(b)

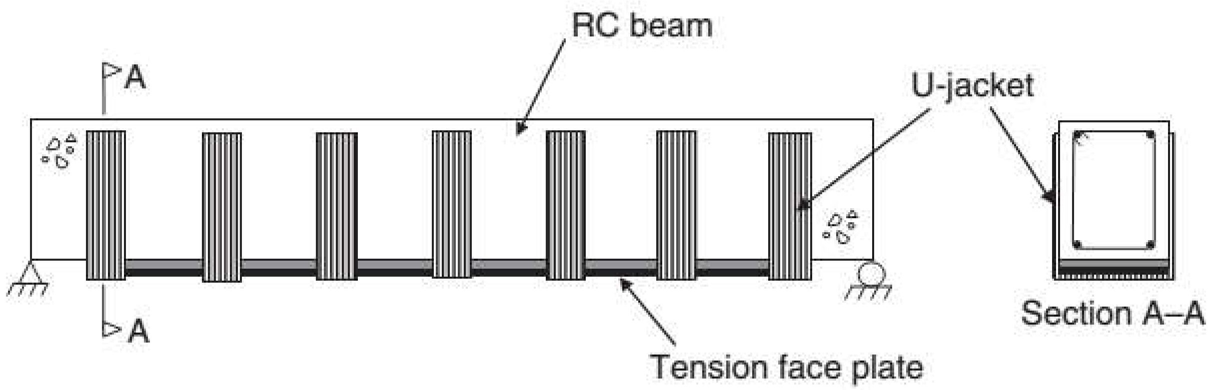

4.19 Combined use of tension face plate and U-jacketing to prevent plate end debonding.

تقویت برشی

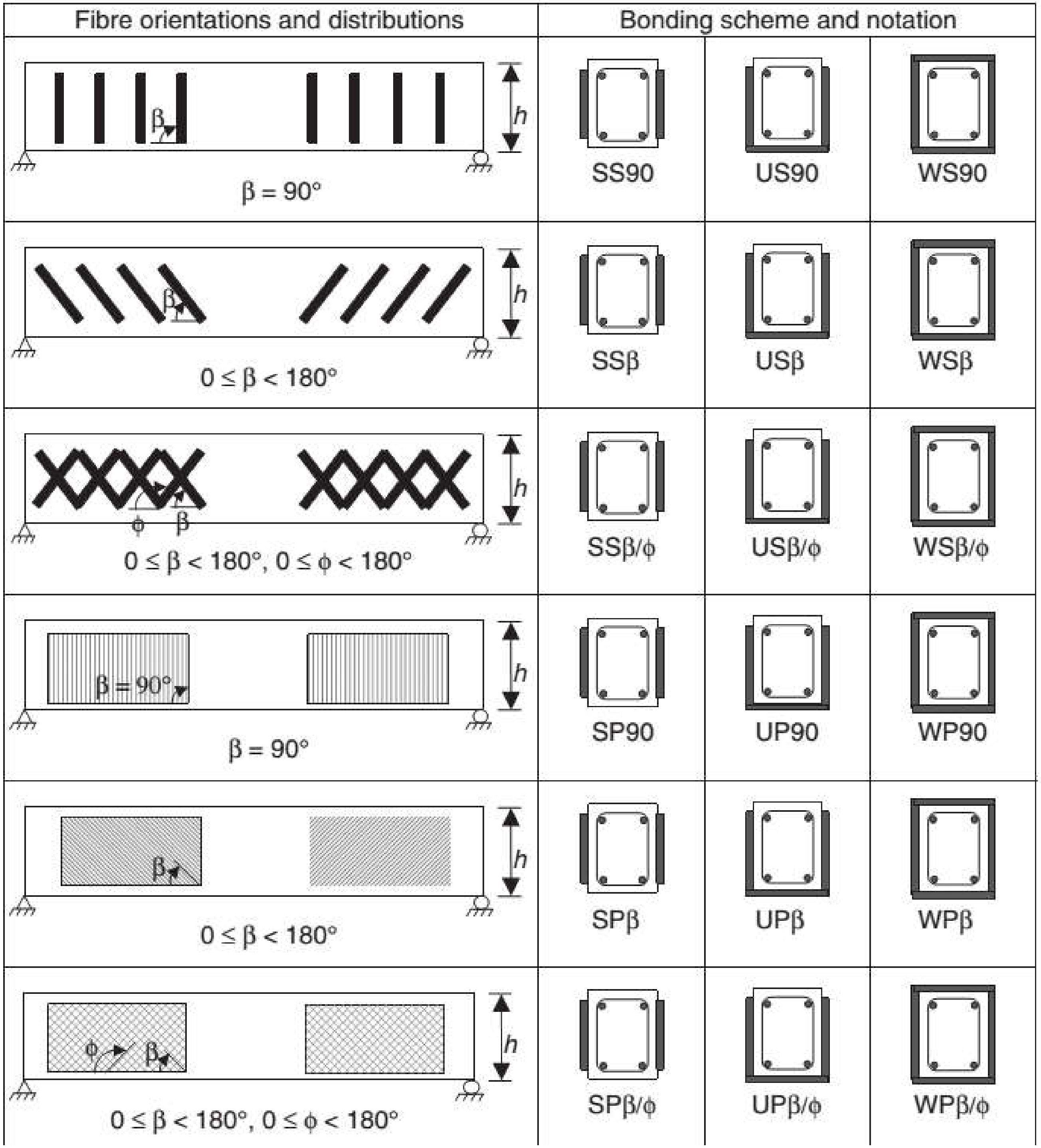
Fibre orientations and distributions
Bonding scheme and notation
β = 90°
SS90
US90
WS90
0 ≤ β < 180°
SSβ
USβ
WSβ
0 ≤ β < 180°, 0 ≤ ϕ < 180°
SSβ/ϕ
USβ/ϕ
WSβ/ϕ
β = 90°
SP90
UP90
WP90
0 ≤ β < 180°
SPβ
UPβ
WPβ
0 ≤ β < 180°, 0 ≤ ϕ < 180°
SPβ/ϕ
UPβ/ϕ
WPβ/ϕ
h

مود شکست برشی

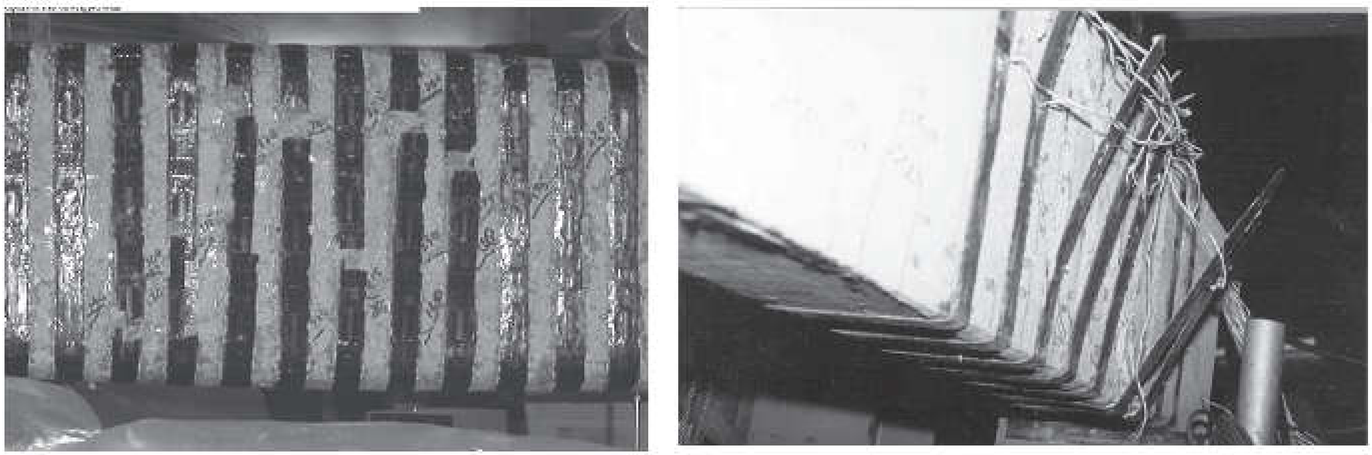

(a) (b)

5.2 Shear failure modes of FRP-strengthened RC beams: (a) rupture of complete FRP wraps; (b) debonding of FRP U-jackets.

تقویت ستون

6.2 Failure of an FRP-confined circular concrete column by FRP rupture.

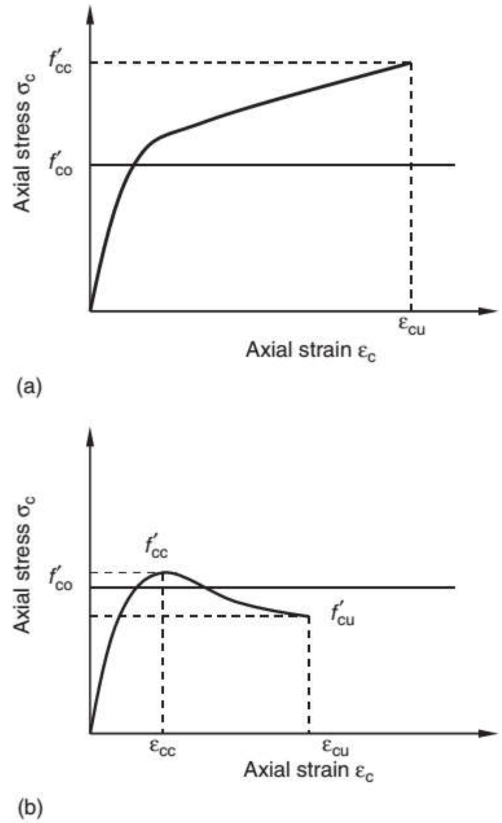

6.3 Typical stress–strain curves of FRP-confined concrete: (a) ascending type; (b) descending type.

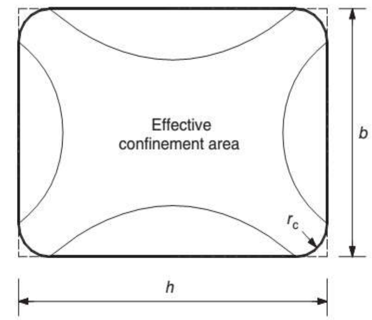

6.10 Effective confinement area of a rectangular section.

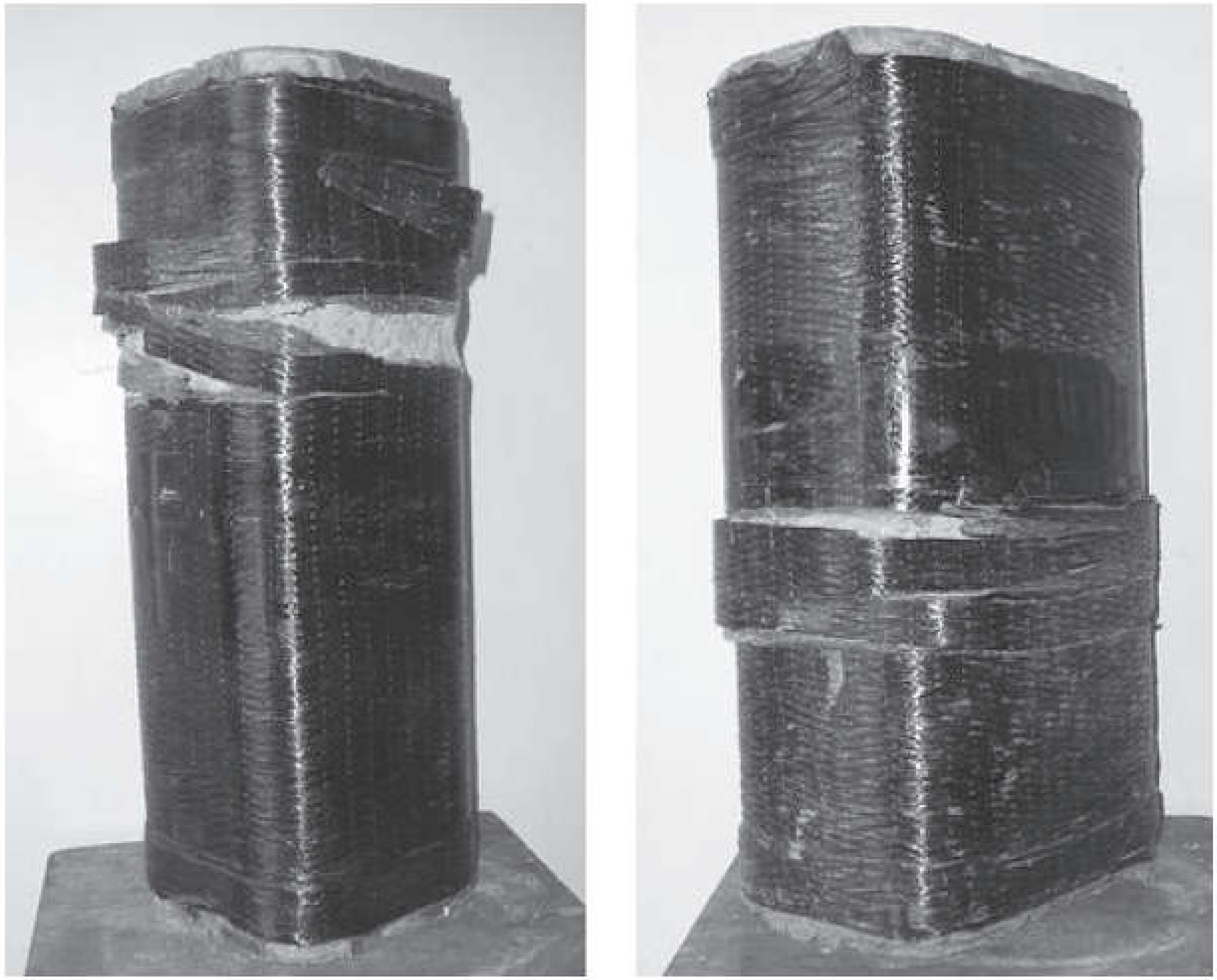

(a) (b)

6.4 Failures of FRP-confined square and rectangular concrete columns with rounded corners by FRP rupture: (a) square column; (b) rectangular column.

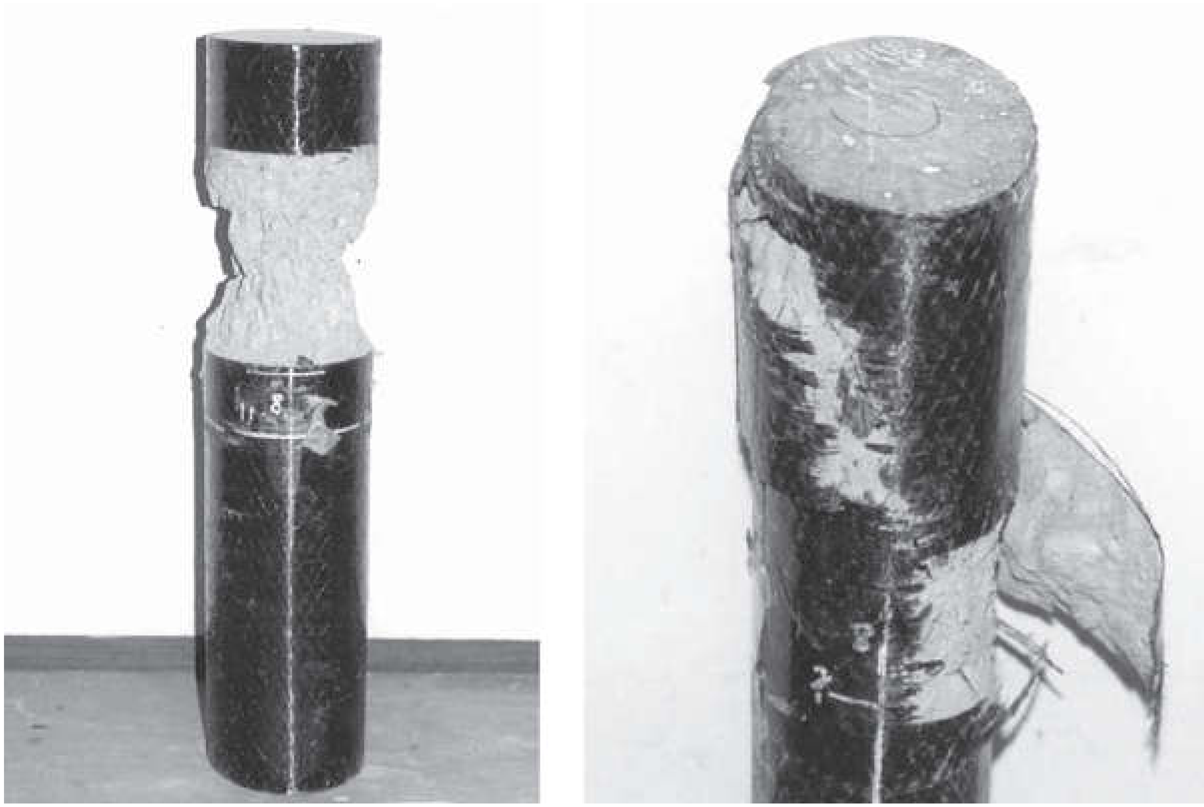

(a) (b)

6.7 Failures of FRP-confined elliptical concrete columns: (a) $a/b = 5/4$; (b) $a/b = 5/3$.

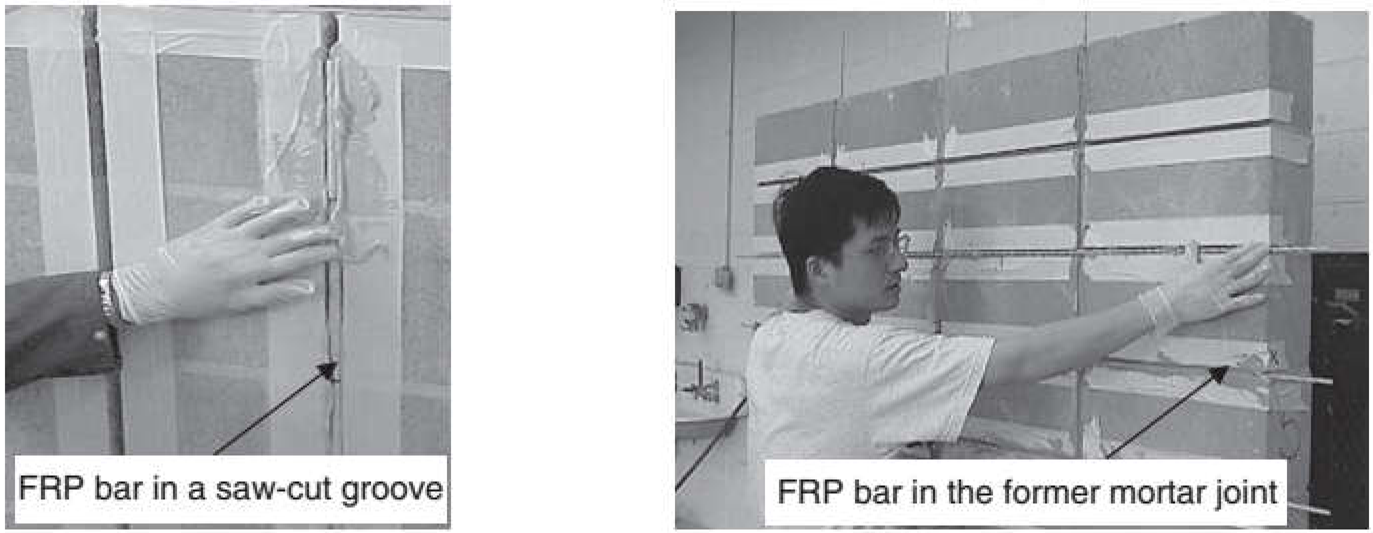

(a) (b)

9.1 Masonry walls strengthened with NSM FRP bars (a) or structural repointing (b) (from Tumialan and Nanni, 2001).

(a) (b)

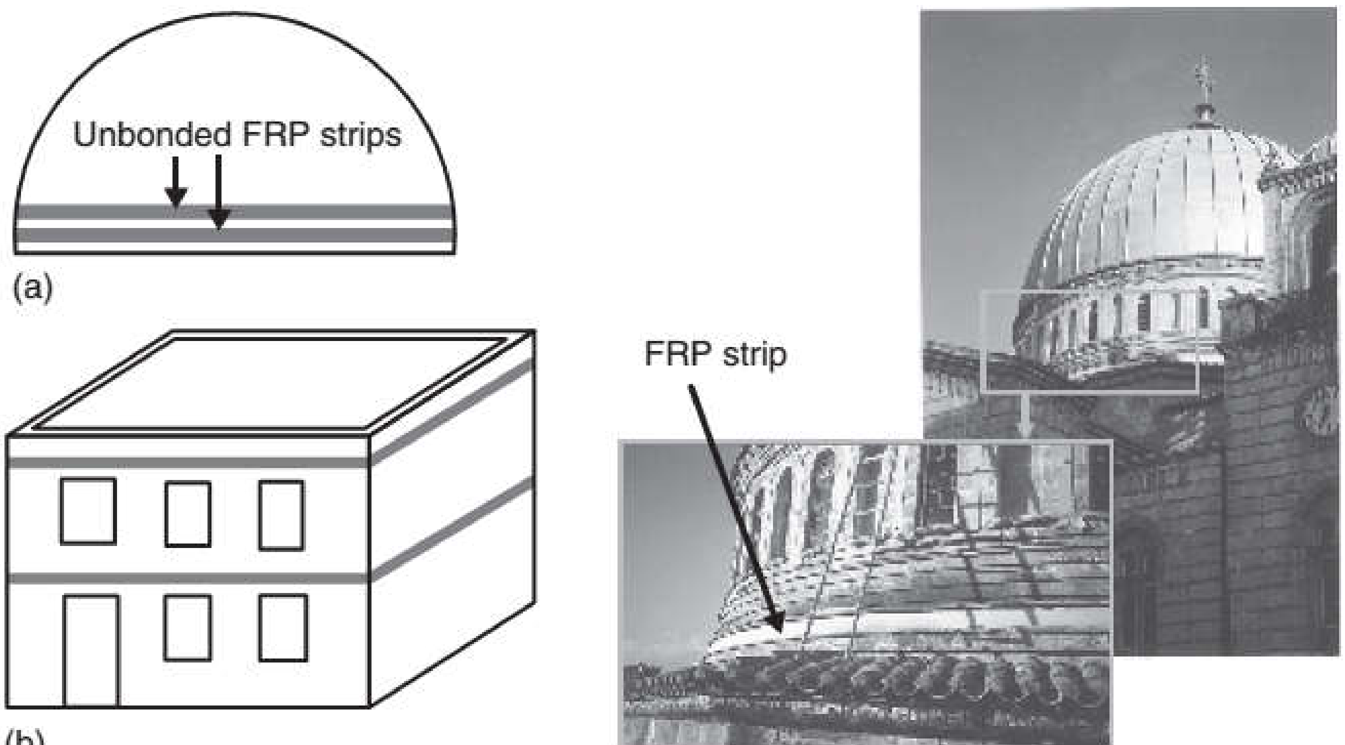

(c)

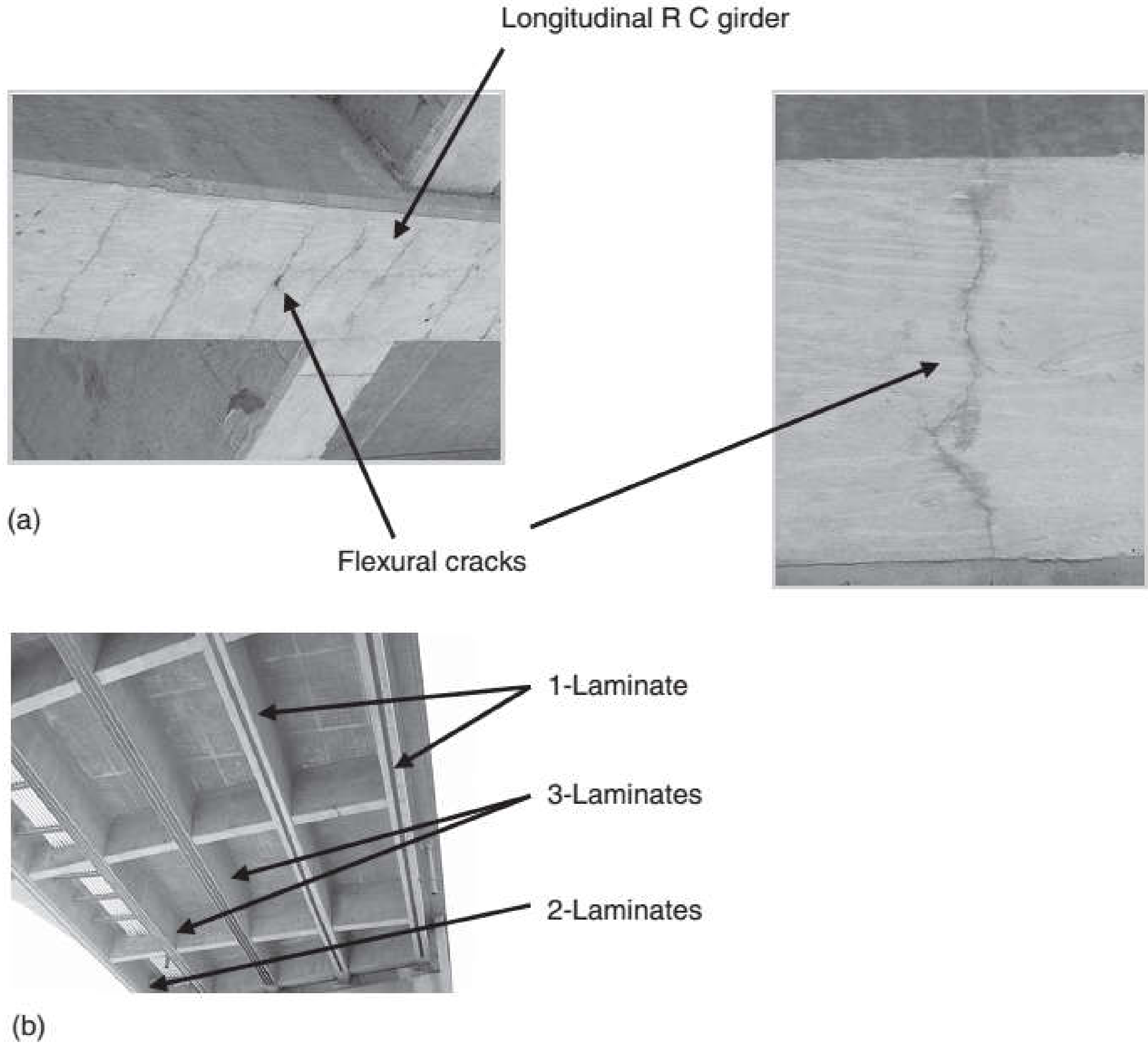

13.1 (a) Visual evidence of damage; (b) completed rehabilitation work in central span (kind permission of Professor I Harik, University of Kentucky, USA).

(a) (b)

13.3 (a) Adhesive FRP plate bonding on cantilever slab; (b) *in situ* FRP fabric lamination on cantilever slab (by kind permission of Mouchel Parkman, West Byfleet, UK).

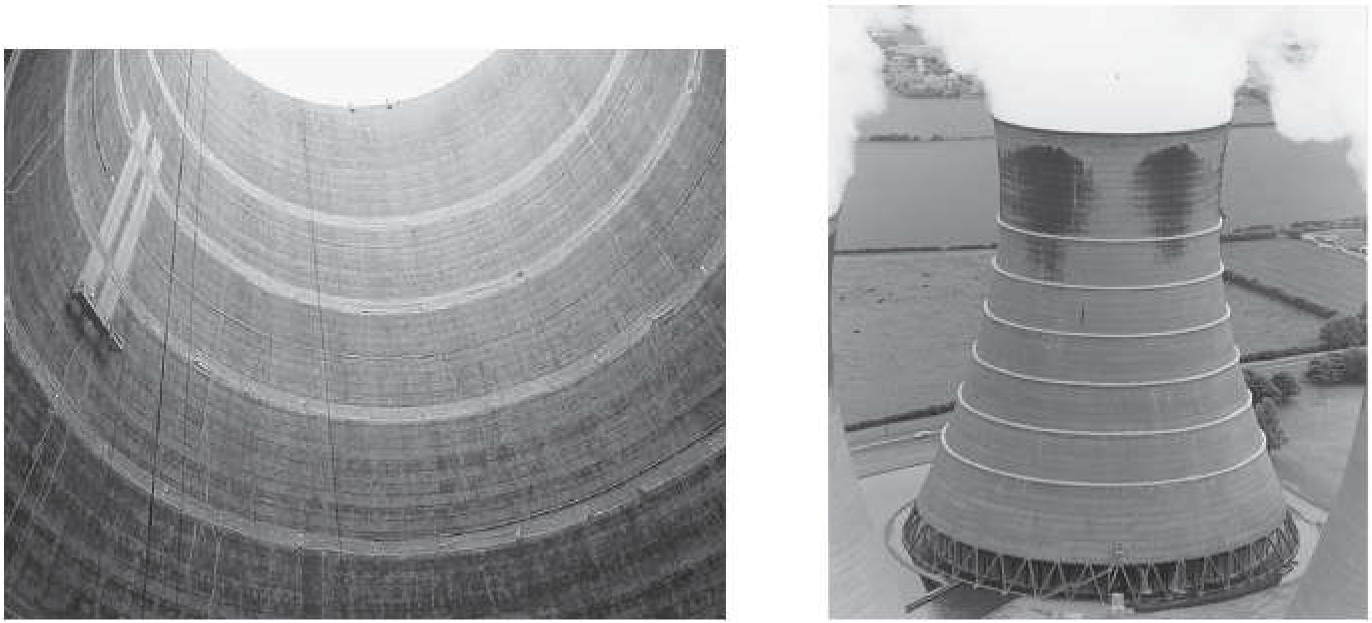

(a) (b)

13.4 Cooling tower Cl, from Doyle *et al.* (2004): (a) bands of aramid fibre strengthening inside of tower; (b) completed tower C1 (by kind permission of Thompson Publishing Services and AA Balkema Publishers).

(a) (b)

13.6 (a) Illustrations of the corroded columns; (b) FRP composite rehabilitation of columns (by kind permission of Concrete International – Neale and Labossière 1998).

13.11 Strengthening masonry wall (photograph by courtesy of Sika Ltd).